Multi-periodic boundary conditions and the Contact Dynamics method

Farhang Radjai

C. R. Mecanique 346 (2018) 263–277

Contents lists available at ScienceDirect

Comptes Rendus Mecanique

www.sciencedirect.com

The legacy of Jean-Jacques Moreau in mechanics

Multi-periodic boundary conditions and the Contact Dynamics method

Farhang Radjai [a,b,*]

[a] LMGC, CNRS–University of Montpellier, 163, rue Auguste-Broussonnet, 34090 Montpellier, France
[b] MultiScale Material Science for Energy and Environment, UMI 3466 CNRS–MIT, Massachusetts Institute of Technology, 77 Massachusetts Avenue, Cambridge 02139, USA

ARTICLE INFO

Article history:
Received 20 May 2017
Accepted 11 October 2017
Available online 27 December 2017

Keywords:
Granular materials
Contact Dynamics method
Periodic boundary conditions

ABSTRACT

For investigating the mechanical behavior of granular materials by means of the discrete element approach, it is desirable to be able to simulate representative volume elements with macroscopically homogeneous deformations. This can be achieved by means of fully periodic boundary conditions such that stresses or displacements can be applied in all space directions. We present a general framework for periodic boundary conditions in granular materials and its implementation more specifically in the Contact Dynamics method.

1. Introduction

Granular materials are of primary importance in a variety of scientific and technological areas such as soil mechanics, geological processes and flows, soft matter physics, powder technology and agronomy. Frictional-contact interactions between particles and physical and/or chemical effects of an interstitial fluid or solid material lead to a nonlinear rheological behavior that has not yet been fully formulated in the framework of a continuum theory. In particular, the state variables in quasi-static and/or inertial granular flows and their evolution with shear strain reflect the complex evolution of the contact network, and still need to be clearly identified and included in a continuum description of the plastic behavior.

The particle-scale variables have been a subject of constant experimental investigation for fifty years, and many features pertaining to the contact network such as fabric anisotropy and force distributions have been analyzed. This move towards particle-scale modeling was later reinforced by the application of the Discrete Element Method (DEM) for the simulation of particle dynamics [1–12]. The DEM is based on the step-wise integration of the equations of motion for all particles, described as rigid elements, by accounting for contact interactions and boundary conditions. The DEM can also be seen as an application of the Molecular Dynamics (MD) method to rigid particles. The perfectly rigid nature of the particles involves only the rigid-body degrees of freedom, but the application of classical explicit integration methods requires a regular (smooth) *force law* at the contact point between two particles with a *contact deflection* defined from their overlap. Generally, the repulsive force is considered to be proportional to the overlap and a viscous damping term is added to account for inelastic collisions.

A new approach to the DEM emerged from a mathematical formulation of nonsmooth dynamics and algorithmic developments by J.-J. Moreau and M. Jean [13–21]. This approach, called Contact Dynamics (CD), is based on a nonsmooth

* Correspondence to: LMGC, CNRS–University of Montpellier, 163, rue Auguste-Broussonnet, 34090 Montpellier, France.
E-mail address: franck.radjai@umontpellier.fr.

https://doi.org/10.1016/j.crme.2017.12.007

formulation of particle dynamics in the sense that the particle velocities and contact forces are simultaneously computed at each time step from the balance of momenta by taking into account the unilateral contact interactions and Coulomb friction law, hence without introducing contact deflection and a repulsive potential. The CD method has been applied to investigate granular materials [22–29,9,30–33], as well as masonry and tensegrity structures [34,35]. For static and plastic shear properties, the CD simulations agree well with MD simulations [36,22,37–40]. The main difference between the two methods in their application to granular materials is the resolution of elastic time scales in the MD method in contrast to the CD method, in which the natural time unit is imposed by particle dynamics and external actions [37,9,41].

The application of the DEM for the investigation of the rheology of granular materials is hindered by the relatively low number of numerically tractable particles as compared to that in real materials. In most reported DEM simulations both in 2D and 3D, the number of particles is below 10^4, as a result of the restrictions imposed by available computation power and memory. As a consequence, the numerical samples are not always statistically representative of the bulk behavior but are also influenced by spurious wall effects. The packing fraction is generally lower in the vicinity of rigid walls and wall-induced ordering can deeply propagate into the bulk. The distortion of a confining walls can also lead to arching at the corners and generate stress gradients over long distances inside the numerical sample [42]. Such effects are real and arise also naturally in experiments on granular materials. However, the number of particles in experiments is generally much higher and hence the wall effects are more critical in numerical simulations.

The undesired effects of wall-like boundaries can be removed by means of periodic boundary conditions. The simulation domain under periodic conditions becomes a unit cell containing the particles with periodic replica of the cell and its particles paving the whole space. Hence, the particles belonging to the borders of the cell interact only with other particles inside the cell or with their images in the neighboring image cells; see Fig. 4. As a result, the periodic conditions extend the system boundaries to the infinity and the simulation cell simply plays the role of a coordinate system locating particle positions [43]. In other words, the origin of the coordinates becomes immaterial so that the resulting dynamics is invariant by translation and therefore necessarily homogeneous.

In this paper, we present a detailed description of the formulation of periodic boundary conditions for the CD method. Such an extension of the method to periodic boundaries is not theoretically straightforward as it involves periodicity not only in particles positions but also in nonaffine particle velocities and in equations of dynamics. A consistent and general formulation should allow for the application of either stresses or displacements in all directions of space. To do so, the role of the walls should be replaced by the collective degrees of freedom carried by the coordinate system. In this way, the basis vectors become dynamic variables, and their conjugate stresses are expressed as a state function of the granular configuration. This method was first introduced by Parrinello and Rahman for a Hamiltonian conservative system [44]. We extend this approach to granular materials, which are not generally conservative systems as a result of frictional and collisional inelastic dissipation.

In the following, we first introduce the CD method. Then, we consider in detail the kinematics, equations of dynamics and time-stepping schemes under periodic boundary conditions. Finally, we show how the equations of contact dynamics should be modified under periodic boundary conditions. We conclude with a few remarks about the implementation.

2. Contact Dynamics method

2.1. Contact laws

Consider two particles i and j touching at a contact point κ inside a granular material. We assume that a unique common line (here in 2D) tangent to the two particles at κ can be defined. The contact can therefore be endowed with a local reference frame defined by a unit vector $\vec{n}$ normal to the line and a unit vector $\vec{t}$ along the line. A potential (or prospective) contact exists if the gap δ_n between two particles (partners) is sufficiently small so that a collision may occur between the two particles within a small time interval δt (time step in numerical simulations). If the contact is effective ($\delta_n = 0$), a repulsive (positive) normal force f_n may appear at κ with a value depending on the particle velocities and forces exerted on the two partners by their neighboring particles; see Fig. 1. But if $\delta_n > 0$ (nonzero gap), the contact is not effective and f_n is identically zero. These conditions can also be by the "complementarity relations" $\delta_n \geq 0$, $f_n \geq 0$ and $\delta_n f_n = 0$ or cast into the following Signorini's inequalities:

$$\begin{cases} \delta_n > 0 & \Rightarrow \quad f_n = 0 \\ \delta_n = 0 & \Rightarrow \quad f_n \geq 0 \end{cases} \tag{1}$$

Obviously, this relation can not be reduced to a (mono-valued) functional dependence between δ_n and f_n.

The above conditions imply that the normal force vanishes when the contact is not effective. However, the normal force may also vanish at an effective contact. This is the case for $u_n = \dot{\delta}_n > 0$, i.e. for incipient opening of a contact. Otherwise, the effective contact is *persistent*, and we have $u_n = \dot{\delta}_n = 0$. Hence, Signorini's inequalities can be extended as follows:

$$\begin{cases} \delta_n > 0 \Rightarrow f_n = 0 \\ \delta_n = 0 \ \wedge \ \begin{cases} u_n > 0 & \Rightarrow \quad f_n = 0 \\ u_n = 0 & \Rightarrow \quad f_n \geq 0 \end{cases} \end{cases} \tag{2}$$

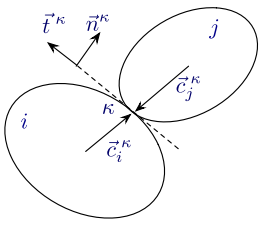

Fig. 1. A contact κ between two particles i and j with contact vectors $\vec{c}_i^{\kappa}$ and $\vec{c}_j^{\kappa}$, and contact frame $(\vec{n}^{\kappa}, \vec{t}^{\kappa})$.

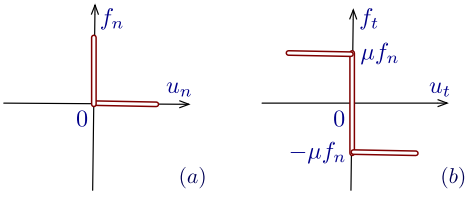

Fig. 2. Graphs of (a) Signorini's inequalities and (b) Coulomb's friction law.

This means that for $\delta_{\rm n} = 0$, Signorini's inequalities hold between the variables $u_{\rm n}$ and $f_{\rm n}$.

In the same way, the Coulomb friction law at an effective contact can be expressed by a set of inequalities for the friction force $f_{\rm t}$ and sliding velocity $u_{\rm t}$:

$$\begin{cases} u_{\rm t} > 0 & \Rightarrow \quad f_{\rm t} = -\mu f_{\rm n} \\ u_{\rm t} = 0 & \Rightarrow \quad -\mu f_{\rm n} \le f_{\rm t} \le \mu f_{\rm n} \\ u_{\rm t} < 0 & \Rightarrow \quad f_{\rm t} = \mu f_{\rm n} \end{cases} \tag{3}$$

where μ is the friction coefficient. It is assumed that the unit tangent vector $\boldsymbol{t}$ points in the direction of sliding velocity such that $\vec{u}_{\rm t} \cdot \vec{t} = u_{\rm t}$. Coulomb's friction law can not be reduced to a (mono-valued) functional dependence between $u_{\rm t}$ and $f_{\rm t}$.

Fig. 2 displays Signorini's inequalities (2) and Coulomb's friction law (3) for an effective contact. The force laws employed in MD may be considered as regularizations of the above contact laws with their vertical branches replaced by steep linear or nonlinear functions.

The use of 'nonsmooth' contact laws in the CD method is consistent with a discrete model of particle motions involving no sub-particle length scale or inherent force scale. But such a coarse model of particle motion implies *nonsmooth dynamics*, i.e. possible discontinuities in particle velocities and forces due to collisions and variations of the contact network. Hence, the approximation of the contact force $f_{\rm n}$ during a time step δt is a measure problem in the mathematical sense [18,45]. A resolved force f^s is the density of the measure $f^s\,{\rm d}t$ with respect to time differential ${\rm d}t$. In contrast, an impulse p generated by a collision has no density with respect to ${\rm d}t$. In other words, the forces at the origin of the impulse are not resolved at the scale δt. In practice, however, we do not differentiate between these contributions in a coarse (particle-scale) dynamics, and the two contributions sum up to a single measure. The contact force is defined as the average of this measure over δt.

In a similar vein, the left velocities $u_{\rm n}^-$ and $u_{\rm t}^-$ at time t are not always related by a smooth variation (acceleration multiplied by time step δt) with the right velocities $u_{\rm n}^+$ and $u_{\rm t}^+$ at $t + \delta t$. Hence, the contact laws (2) and (3) are assumed to be satisfied for a weighted mean of the left and right contact velocities:

$$u_{\rm n} = \frac{u_{\rm n}^+ + e_{\rm n}\, u_{\rm n}^-}{1 + e_{\rm n}} \tag{4}$$

$$u_{\rm t} = \frac{u_{\rm t}^+ + e_{\rm t}\, u_{\rm t}^-}{1 + |e_{\rm t}|} \tag{5}$$

For a binary collision, the normal force is nonzero, and Signorini's graph implies $u_{\rm n} = 0$. Therefore, we have $-u_{\rm n}^+/u_{\rm n}^- = e_{\rm n}$, and $e_{\rm n}$ represents the normal restitution coefficient. In the same way, for $u_{\rm t} = 0$, corresponding to a non-sliding contact, we have $-u_{\rm t}^+/u_{\rm t}^- = e_{\rm t}$, that coincides with the tangential restitution coefficient. We see that, when Signorini's and Coulomb's graphs are used with the formal velocities given by equations (4) and (5), a contact is persistent ($u_{\rm n}^+ = 0$) only if $e_{\rm n} = 0$.

In a dense granular flow, the collisions are not binary, and the generated impulses propagate through the contact network. For this reason, a contact may experience many successive impulses during δt. Such events can be resolved for a sufficiently small time interval δt or tracked by means of an event-driven scheme. However, this strategy is numerically inefficient, and contradicts the spirit of the CD method based on coarse-time dynamics. Hence, the use of intermediate velocities (12) with contact laws is a generalization of restitution coefficients to multiple collisions and contact networks. In

this model, the right velocities $u_{\rm n}^+$ and $u_{\rm t}^+$ (at the end of a time step) are not given by the left velocities multiplied by the coefficients of restitution as in binary collisions but by combining the contact laws with equations of dynamics.

2.2. Nonsmooth dynamics

The particle motions are governed by the Newton–Euler equations under the action of external bulk or boundary forces $\vec{F}_{\rm ext}$, and the contact forces $\vec{f}^{\kappa}$ exerted by neighboring particles at the contact points κ. Let unit vectors $(\hat{x},\ \hat{y})$ represent a reference frame in the plane and $\hat{z}=\hat{x}\times\hat{y}$ be the normal to the plane. Each particle is characterized by its mass m, moment of inertia I, mass center coordinates $\vec{r}$, mass center velocity $\vec{U}$, angular coordinates θ with respect to $\hat{z}$, and angular velocity $\omega\hat{z}$. For a smooth motion (twice differentiable), the equations of motion of a particle are

$$\begin{array}{rcl} m\,\dot{\vec{U}} &=& \vec{F}+\vec{F}_{\rm ext} \\ I\,\dot{\omega} &=& \mathcal{M}+\mathcal{M}_{\rm ext} \end{array} \tag{6}$$

where $\vec{F}=\sum_\kappa \vec{f}^{\kappa}$ and $\mathcal{M}=\hat{z}\cdot\sum_\kappa \vec{c}^{\kappa}\times\vec{f}^{\kappa}$ where $\vec{c}^{\kappa}$ is the *contact vector* joining the center of mass to the contact κ and $\mathcal{M}_{\rm ext}$ represents the moment of external forces.

For a nonsmooth motion with time resolution δt involving impulses and velocity jumps, an integrated form of the equations of dynamics should be used. Hence, the equations of dynamics should be written as an equality of measures:

$$\begin{array}{rcl} m\,{\rm d}\vec{U} &=& {\rm d}\vec{F}'+\vec{F}_{\rm ext}\,{\rm d}t \\ I\,{\rm d}\omega &=& {\rm d}\mathcal{M}'+\mathcal{M}_{\rm ext}\,{\rm d}t \end{array} \tag{7}$$

where ${\rm d}\vec{F}'=\sum_\kappa {\rm d}\vec{f}'^{\kappa}$ and ${\rm d}\mathcal{M}'=\hat{z}\cdot\sum_\kappa \vec{c}^{\kappa}\times{\rm d}\vec{f}'^{\kappa}$. These measure equations can be integrated over δt with $\vec{F}$ and $\mathcal{M}$ as approximations of the integral of ${\rm d}\vec{F}'$ and ${\rm d}\mathcal{M}'$. With these definitions, we have

$$\begin{array}{rcl} m\,(\vec{U}^+-\vec{U}^-) &=& \delta t\,\vec{F}+\delta t\,\vec{F}_{\rm ext} \\ I\,(\omega^+-\omega^-) &=& \delta t\,\mathcal{M}+\delta t\,\mathcal{M}_{\rm ext} \end{array} \tag{8}$$

where $(\vec{U}^-,\omega^-)$ and $(\vec{U}^+,\omega^+)$ are the left and right velocities of the particle, respectively, at each time step.

The equations of dynamics can be written in matrix form for a set of $N_{\rm p}$ particles labeled with integers $i\in[1,N_{\rm p}]$. The forces and force moments F_x^i, F_y^i, $\mathcal{M}^i$ acting on the particles i are arranged in a column vector represented by a boldface letter $\mathbf{F}$ and belonging to $\mathbb{R}^{3N_{\rm p}}$. In the same way, the external bulk forces $F_{{\rm ext},x}$, $F_{{\rm ext},y}$, $\mathcal{M}_{\rm ext}$ applied on the particles and the particle velocity components U_x^i, U_y^i, ω^i are represented by column vectors $\mathbf{F}_{\rm ext}$ and $\mathbf{U}$, respectively. The particle masses and moments of inertia define a diagonal $3N_{\rm p}\times 3N_{\rm p}$ matrix denoted by $\mathbf{M}$. With these notations, the equations of dynamics (8) are represented by the matrix equation

$$\mathbf{M}(\mathbf{U}^+-\mathbf{U}^-)=\delta t(\mathbf{F}+\mathbf{F}_{\rm ext}) \tag{9}$$

2.3. Contact dynamics equations

Since the contact laws involve contact variables ($u_{\rm n}$, $u_{\rm t}$, $f_{\rm n}$ and $f_{\rm t}$), we need to express the equations (9) in terms of the same variables. The contacts are labeled with integers $\kappa\in[1,N_{\rm c}]$, where $N_{\rm c}$ is the total number of contacts. Like particle velocities, the contact velocities $u_{\rm n}^{\kappa}$ and $u_{\rm t}^{\kappa}$ can be collected in a column vector $\mathbf{u}\in\mathbb{R}^{2N_{\rm c}}$. In the same way, the contact forces $f_{\rm n}^{\kappa}$ and $f_{\rm t}^{\kappa}$ are represented by a vector $\mathbf{f}\in\mathbb{R}^{2N_{\rm c}}$. We would like to express the equations of dynamics in terms of $\mathbf{f}$ and $\mathbf{u}$. Since the contact velocities $\mathbf{u}$ are linear in particle velocities $\mathbf{U}$, the transformation of the velocities is an affine application:

$$\mathbf{u}=\mathbf{G}\,\mathbf{U} \tag{10}$$

where $\mathbf{G}$ is a $2N_{\rm c}\times 3N_{\rm p}$ matrix carrying the information on the geometry of the contact network. A similar linear application relates $\mathbf{f}$ to $\mathbf{F}$:

$$\mathbf{F}=\mathbf{H}\,\mathbf{f} \tag{11}$$

where $\mathbf{H}$ is a $3N_{\rm p}\times 2N_{\rm c}$ matrix. We refer to $\mathbf{H}$ as a *contact matrix*. It contains the same information as $\mathbf{G}$. It can be shown that $\mathbf{H}=\mathbf{G}^{\mathsf{T}}$ where $\mathbf{G}^{\mathsf{T}}$ is the transpose of $\mathbf{G}$. This property can be inferred from the equivalence between the power $\mathbf{F}\cdot\mathbf{U}$ developed by "generalized" forces $\mathbf{F}$ and the power $\mathbf{f}\cdot\mathbf{u}$ developed by the bond forces $\mathbf{f}$. In general, the matrix $\mathbf{H}$ is singular and, by definition, its null space has a dimension at least equal to $2N_{\rm c}-3N_{\rm p}$.

The matrix $H^{i\kappa}$ can be partitioned into two matrices $H_{\rm n}^{i\kappa}$ and $H_{\rm t}^{i\kappa}$ such that

$$\begin{array}{rcl} u_{\rm n}^{\kappa} &=& \displaystyle\sum_i H_{\rm n}^{{\mathsf{T}},\kappa i}\,U^i \\ u_{\rm t}^{\kappa} &=& \displaystyle\sum_i H_{\rm t}^{{\mathsf{T}},\kappa i}\,U^i \end{array} \tag{12}$$

and

$$F^i = \sum_\kappa (H_{\rm n}^{i\kappa}\ f_{\rm n}^\kappa + H_{\rm t}^{i\kappa}\ f_{\rm t}^\kappa) \tag{13}$$

Using these relations, (9) can be transformed into two equations for each contact κ:

$$\begin{aligned} u_{\rm n}^{\kappa+} - u_{\rm n}^{\kappa-} &= \delta t \sum_{i,j} H_{\rm n}^{\mathsf{T},\kappa i}\, M^{-1,ij} \\ &\quad \{\sum_\lambda (H_{\rm n}^{j\lambda} f_{\rm n}^\lambda + H_{\rm t}^{j\lambda} f_{\rm t}^\lambda) + F_{\rm ext}^j\} \\ u_{\rm t}^{\kappa+} - u_{\rm t}^{\kappa-} &= \delta t \sum_{i,j} H_{\rm t}^{\mathsf{T},\kappa i}\, M^{-1,ij} \\ &\quad \{\sum_\lambda (H_{\rm n}^{j\lambda} f_{\rm n}^\lambda + H_{\rm t}^{j\lambda} f_{\rm t}^\lambda) + F_{\rm ext}^j\} \end{aligned} \tag{14}$$

We now can write down explicit linear relations between the contact variables from equations (14) and (12). Let us set

$$\mathcal{W}_{k_1k_2}^{\kappa\lambda} = \sum_{i,j} H_{k_1}^{\mathsf{T},\kappa i} M^{-1,ij} H_{k_2}^{j\lambda}, \tag{15}$$

where k_1 and k_2 stand for n or t. With this notation, (14) can be rewritten as

$$\begin{aligned} \frac{1+e_{\rm n}}{\delta t}\,(u_{\rm n}^\kappa - u_{\rm n}^{\kappa-}) &= \mathcal{W}_{\rm nn}^{\kappa\kappa} f_{\rm n}^\kappa + \mathcal{W}_{\rm nt}^{\kappa\kappa} f_{\rm t}^\kappa \\ &\quad + \sum_{\lambda(\neq\kappa)} \{\mathcal{W}_{\rm nn}^{\kappa\lambda} f_{\rm n}^\lambda + \mathcal{W}_{\rm nt}^{\kappa\lambda} f_{\rm t}^\lambda\} \\ &\quad + \sum_{i,j} H_n^{\mathsf{T},\kappa i} M^{-1,ij} F_{\rm ext}^j \end{aligned} \tag{16}$$

$$\begin{aligned} \frac{1+e_{\rm t}}{\delta t}\,(u_{\rm t}^\kappa - u_{\rm t}^{\kappa-}) &= \mathcal{W}_{\rm tn}^{\kappa\kappa} f_{\rm n}^\kappa + \mathcal{W}_{\rm tt}^{\kappa\kappa} f_{\rm t}^\kappa \\ &\quad + \sum_{\lambda(\neq\kappa)} \{\mathcal{W}_{\rm tn}^{\kappa\lambda} f_{\rm n}^\lambda + \mathcal{W}_{\rm nt}^{\kappa\lambda} f_{\rm t}^\lambda\} \\ &\quad + \sum_{i,j} H_t^{\mathsf{T},\kappa i} M^{-1,ij} F_{\rm ext}^j \end{aligned} \tag{17}$$

The coefficients $\mathcal{W}_{k_1k_2}^{\kappa\kappa}$ for each contact κ can be calculated from the contact network geometry and inertia parameters of the two partners 1_κ and 2_κ of the contact κ. Let $\vec{c}_i^{\,\kappa}$ be the contact vector joining the center of mass of particle i to the contact κ. We get

$$\begin{aligned} \mathcal{W}_{\rm nn}^{\kappa\kappa} &= \frac{1}{m_{1_\kappa}} + \frac{1}{m_{2_\kappa}} + \frac{(c_{1t}^\kappa)^2}{I_{1_\kappa}} + \frac{(c_{2t}^\kappa)^2}{I_{2_\kappa}} \\ \mathcal{W}_{\rm tt}^{\kappa\kappa} &= \frac{1}{m_{1_\kappa}} + \frac{1}{m_{2_\kappa}} + \frac{(c_{1n}^\kappa)^2}{I_{1_\kappa}} + \frac{(c_{2n}^\kappa)^2}{I_{2_\kappa}} \\ \mathcal{W}_{\rm nt}^{\kappa\kappa} &= \mathcal{W}_{\rm tn}^{\kappa\kappa} = \frac{c_{1n}^\kappa c_{1t}^\kappa}{I_{1_\kappa}} + \frac{c_{2n}^\kappa c_{2t}^\kappa}{I_{2_\kappa}} \end{aligned} \tag{18}$$

where $c_{i\,\rm n}^\kappa = \vec{c}_i^{\,\kappa} \cdot \vec{n}^\kappa$ and $c_{i\,\rm t}^\kappa = \vec{c}_i^{\,\kappa} \cdot \vec{t}^\kappa$ are the components of the contact vectors in the contact frame. The coefficients $\mathcal{W}_{k_1k_2}^{\kappa\kappa}$ are inverse reduced inertia.

An alternative representation of equations (16) and (17) is

$$\mathcal{W}_{\rm nn}^{\kappa\kappa} f_{\rm n}^\kappa + \mathcal{W}_{\rm nt}^{\kappa\kappa} f_{\rm t}^\kappa = (1+e_{\rm n})\,\frac{1}{\delta t} u_{\rm n}^\kappa + a_{\rm n}^\kappa \tag{19}$$

$$\mathcal{W}_{\rm tt}^{\kappa\kappa} f_{\rm t}^\kappa + \mathcal{W}_{\rm tn}^{\kappa\kappa} f_{\rm n}^\kappa = (1+e_{\rm t})\,\frac{1}{\delta t} u_{\rm t}^\kappa + a_{\rm t}^\kappa \tag{20}$$

The two offsets $a_{\rm n}^\kappa$ and $a_{\rm t}^\kappa$ can be expressed from equations (16) and (17). We refer to equations (19) and (20) or, equivalently, to equations (16) and (17) as *contact dynamics equations* as they replace the equations of dynamics in terms of contact variables [46].

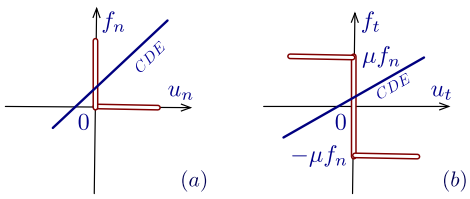

Fig. 3. Solution of the local equations of dynamics obtained from the intersection between contact dynamics equations (CDE) and the Signorini and Coulomb contact laws.

The two terms a_n and a_t are given by the following expressions:

$$a_\mathrm{n}^\kappa = b_\mathrm{n}^\kappa - (1+e_\mathrm{n})\frac{1}{\delta t}\,u_\mathrm{n}^{\kappa-} + \left(\frac{\vec{F}_{\mathrm{ext}}^{2_\kappa}}{m_{2_\kappa}} - \frac{\vec{F}_{\mathrm{ext}}^{1_\kappa}}{m_{1_\kappa}}\right)\cdot\vec{n}^\kappa \tag{21}$$

$$a_\mathrm{t}^\kappa = b_\mathrm{t}^\kappa - (1+e_\mathrm{t})\frac{1}{\delta t}\,u_\mathrm{t}^{\kappa-} + \left(\frac{\vec{F}_{\mathrm{ext}}^{2_\kappa}}{m_{2_\kappa}} - \frac{\vec{F}_{\mathrm{ext}}^{1_\kappa}}{m_{1_\kappa}}\right)\cdot\vec{t}^\kappa \tag{22}$$

The contribution of left velocities $(u_\mathrm{n}^{\kappa-}, u_\mathrm{t}^{\kappa-})$ appears in these equations as an impulse depending on the reduced mass and the restitution coefficient. The contribution of contact forces $\vec{f}_i^{\,\lambda}$ acting on the two touching particles are represented by the terms b_n^κ and b_t^κ given by

$$b_\mathrm{n}^\kappa = \frac{1}{m_{2_\kappa}}\sum_{\lambda(\neq\kappa)}\vec{f}_{2_\kappa}^{\,\lambda}\cdot\vec{n}^\kappa - \frac{1}{m_{1_\kappa}}\sum_{\lambda(\neq\kappa)}\vec{f}_{1_\kappa}^{\,\lambda}\cdot\vec{n}^\kappa \tag{23}$$

$$b_\mathrm{t}^\kappa = \frac{1}{m_{2_\kappa}}\sum_{\lambda(\neq\kappa)}\vec{f}_{2_\kappa}^{\,\lambda}\cdot\vec{t}^\kappa - \frac{1}{m_{1_\kappa}}\sum_{\lambda(\neq\kappa)}\vec{f}_{1_\kappa}^{\,\lambda}\cdot\vec{t}^\kappa \tag{24}$$

The contact dynamics equations (19) and (20) define a system of two linear equations between the contact variables at each contact point. For given values of a_n and a_t at a contact, the contact laws (2) and (3) should also be satisfied. Hence, the solution is at the intersection between the straight line (19) and Signorini's graph on one hand, and between (20) and Coulomb's graph, on the other hand; see Fig. 3. The intersection occurs at a unique point due to the positivity of the coefficients $\mathcal{W}_{k_1k_2}^{\kappa\kappa}$ (positive slope).

To find the solution, one may consider the intersection of contact dynamics equations with the force axis, i.e. by setting $u_\mathrm{n} = u_\mathrm{t} = 0$. This yields two values g_n^κ and g_t^κ of f_n^κ and f_t^κ, respectively:

$$g_\mathrm{n}^\kappa = \frac{\mathcal{W}_{\mathrm{tt}}^{\kappa\kappa}a_\mathrm{n}^\kappa - \mathcal{W}_{\mathrm{nt}}^{\kappa\kappa}a_\mathrm{t}^\kappa}{\mathcal{W}_{\mathrm{nn}}^{\kappa\kappa}\mathcal{W}_{\mathrm{tt}}^{\kappa\kappa} - (\mathcal{W}_{\mathrm{nt}}^{\kappa\kappa})^2} \tag{25}$$

$$g_\mathrm{t}^\kappa = \frac{\mathcal{W}_{\mathrm{nn}}^{\kappa\kappa}a_\mathrm{n}^\kappa - \mathcal{W}_{\mathrm{tn}}^{\kappa\kappa}a_\mathrm{t}^\kappa}{\mathcal{W}_{\mathrm{tt}}^{\kappa\kappa}\mathcal{W}_{\mathrm{nn}}^{\kappa\kappa} - (\mathcal{W}_{\mathrm{tn}}^{\kappa\kappa})^2} \tag{26}$$

It can be shown that the denominator is positive. If $g_\mathrm{n}^\kappa < 0$, then the solution is $f_\mathrm{n}^\kappa = f_\mathrm{t}^\kappa = 0$. This corresponds to a *breaking contact*. Otherwise, i.e. if $g_\mathrm{n}^\kappa \geq 0$, we have $f_\mathrm{n}^\kappa = g_\mathrm{n}^\kappa$. With this value of f_n^κ, we can determine the solution of the Coulomb problem. If $g_\mathrm{t}^\kappa > \mu f_\mathrm{n}^\kappa$, the solution is $f_\mathrm{t}^\kappa = \mu f_\mathrm{n}^\kappa$ and in the opposite case, i.e. if $g_\mathrm{t}^\kappa < -\mu f_\mathrm{n}^\kappa$, the solution is $f_\mathrm{t}^\kappa = -\mu f_\mathrm{n}^\kappa$ (*sliding contact*). Otherwise, i.e. when $-\mu f_\mathrm{n}^\kappa < g_\mathrm{t}^\kappa < \mu f_\mathrm{n}^\kappa$, the solution is $f_\mathrm{t}^\kappa = g_\mathrm{t}^\kappa$ (*rolling contact*).

2.4. Iterative resolution

To solve the system of $2N_\mathrm{c}$ contact dynamics equations (in 2D) with the corresponding contact laws, we proceed by an iterative method which converges to the solution simultaneously for all contact forces and velocities. In a multi-contact system, the contributions of b_n^κ and b_t^κ to the offsets a_n^κ and a_t^κ depend on the forces and velocities at contacts $\lambda \neq \kappa$; see equations (21), (22), (23) and (24). Hence, the solution for each contact depends on all other contacts of the system and it must be determined simultaneously for all contacts. A robust method consists in searching the solution as the limit of a sequence $\{f_\mathrm{n}^\kappa(k), f_\mathrm{t}^\kappa(k), u_\mathrm{n}^\kappa(k), u_\mathrm{t}^\kappa(k)\}$ with $\kappa \in [1, N_\mathrm{c}]$. Let us assume that a temporary set of contact forces $\{f_\mathrm{n}^\kappa(k), f_\mathrm{t}^\kappa(k)\}$ at iteration step k is given. From this set, the offsets $\{a_\mathrm{n}^\kappa(k), a_\mathrm{t}^\kappa(k)\}$ for all contacts can be calculated through the relations (21) and (22). The local problem can then be solved for each contact κ with these values of the offsets, yielding an updated set of contact forces $\{f_\mathrm{n}^\kappa(k+1), f_\mathrm{t}^\kappa(k+1)\}$.

This force-update procedure does not require the calculation of contact velocities $u_\mathrm{n}^\kappa(k+1), u_\mathrm{t}^\kappa(k+1)\}$ since the offsets depend only on the contact forces. The set $\{f_\mathrm{n}^\kappa(k), f_\mathrm{t}^\kappa(k)\}$ evolves with k by successive corrections and it converges to a solution satisfying the contact dynamics equations and contact laws at all potential contacts of the system. The iteration can

be stopped when the set $\{f_{\rm n}^{\kappa}(k), f_{\rm t}^{\kappa}(k)\}$ is stable with regard to the force update procedure within a prescribed precision criterion ε_f:

$$\frac{\mid f^{\kappa}(k+1) - f^{\kappa}(k) \mid}{f^{\kappa}(k+1)} < \varepsilon_f \quad \forall \kappa \tag{27}$$

Finally, from the converged contact forces, the particle velocities $\{\vec{U}^i\}$ can be computed by means of the equations of dynamics (8).

This iterative procedure provides a robust method which has proven efficient in application to the dynamics of granular materials. The information is treated locally and no large matrices are manipulated during iterations. The number N_i of necessary iterations for convergence depends on the precision ε_f but not on the time step δt. The number of necessary iterations is substantially reduced when the iteration at each time step is initialized with a good guess of the forces such as those computed in the preceding step. We find that to obtain a correct calculation of force distributions, ε_f should be below 10^{-3}. This is particularly true for the large class of forces below the average force [23].

The uniqueness of the solution in a multi-contact system with rigid particles is not guaranteed at each step. There are $3N_{\rm p}$ equations of dynamics and $2N_{\rm c}$ contact relations. The unknown variables are the $3N_{\rm p}$ particle velocities and $2N_{\rm c}$ contact forces. The indeterminacy arises from the fact that the $2N_{\rm c}$ contact relations are *inequations*. Thus, the extent of indeterminacy of the solution reflects all possible combinations of contact forces accommodating the contact inequations. The indeterminacy may be high, but it does not imply significant force variability since the solutions are strongly constrained by contact laws. In practice, as a result of finite numerical precision, the risk of not finding a mechanically admissible solution (satisfying both the contact laws and equations of dynamics) is higher than that of missing the right solution. In other words, the variability of the solution is generally below the precision ε_f when the forces are computed at each time step from the forces at the preceding step.

The time-stepping scheme is based on the fact that Signorini's condition (2) for particle positions is the only condition referring to space coordinates. Both the equations of dynamics and contact laws are formulated at the velocity level, and Signorini's condition for particle positions is accounted for by considering only the *effective contacts* where $\delta_{\rm n} = 0$. Hence, the contact network is defined explicitly from particle positions and it does not evolve during a time step δt. But the iterative determination of forces and velocities is fully implicit, and the right velocities $\{\vec{U}^{i+}, \omega^{i+}\}$ at the end of a time step should be used to increment particle positions.

Let t and $t + \delta t$ be the considered time interval. The configuration $\{\vec{r}^i(t)\}$ and particle velocities $\{\vec{U}^i(t), \omega^i(t)\}$ are given at time t. These velocities coincide with the left velocities $\{\vec{U}^{i-}, \omega^{i-}\}$. The contact network $\{\kappa, \vec{n}^{\kappa}, \vec{t}^{\kappa}\}$ is set up from the particle configuration at time t or from an intermediate configuration $\{\vec{r}_{\rm m}^i\}$ defined by

$$\vec{r}_{\rm m}^i \equiv \vec{r}^i(t) + \frac{\delta t}{2}\,\vec{U}^i(t) \tag{28}$$

When this configuration is used for contact detection, other space-dependent quantities such as the inverse mass parameters $\mathcal{W}_{k_1k_2}^{\kappa\kappa}$ and external forces $\vec{U}_{\rm ext}^i$ should consistently be defined for the same configuration and at the same time $t + \delta t/2$. Then, the forces and velocities are iteratively determined for this configuration, and the right particle velocities $\{\vec{U}^{i+}, \omega^{i+}\}$ are calculated. These are the velocities at the end of the time step $t + \delta t$:

$$\vec{U}^i(t+\delta t) = \vec{U}^{i+} \tag{29}$$

$$\omega^i(t+\delta t) = \omega^{i+} \tag{30}$$

Finally, the positions are updated by integrating the updated velocities:

$$\vec{r}^i(t+\delta t) = \vec{r}_{\rm m}^i + \frac{\delta t}{2}\,\vec{U}^i(t+\delta t) \tag{31}$$

$$\theta^i(t+\delta t) = \theta_{\rm m}^i + \frac{\delta t}{2}\,\omega^i(t+\delta t) \tag{32}$$

This scheme is unconditionally stable due to its inherent implicit time integration. Hence, no damping parameters at any level are needed and the time step δt can be large. The real limit on the time step is imposed by the cumulative round-off errors in particle positions, which are updated from the integration of the velocities. Although the excessive overlaps have no dynamic effect in the CD method, they can falsify the particle configuration and the long-term evolution of the system. This means that the choice of the time step should comply with the necessity of correctly predicting new contacts occurring during the evolution of the system without allowing for excessive overlaps. However, decreasing the time step does not improve the quality of the computations if the convergence criterion is too large. In contrast, in Molecular Dynamics, the time step needs to be small for a more accurate calculation of particle velocities. In this sense, the time step in the CD method is not a precision parameter but a temporal coarse-graining parameter for nonsmooth dynamics. It should be reduced if the impulse dynamics at small time scales is of interest.

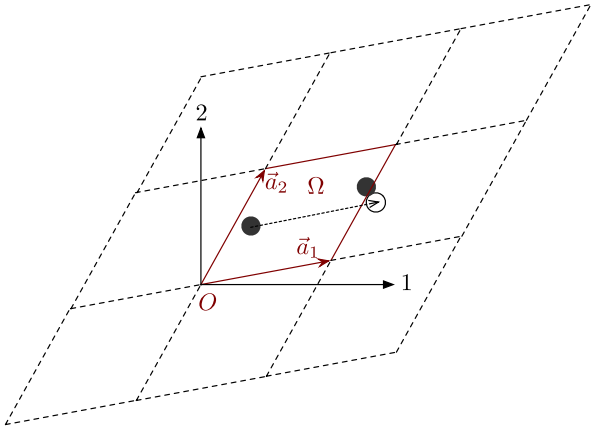

Fig. 4. A 2D simulation cell Ω with its basis vectors.

3. Periodic boundary conditions

In this section, we introduce a general method for the implementation of periodic boundary conditions. We assume here a three-dimensional system but the formalism can naturally be restricted to two dimensions

3.1. Kinematics

Let us consider N_p particles with their centers contained in a cell Ω of volume V. The cell can have any shape compatible with a periodic tessellation of space. The simplest shape is a parallelogram in 2D. Other shapes such as hexagons are equally possible [43]. The cell Ω and its replicas define a regular lattice characterized by its basis vectors $(\vec{a}_1, \vec{a}_2, \vec{a}_3)$. In the case of a parallelepiped, the basis vectors may simply be the three sides of the parallelepiped; see Fig. 4. The origin O of the simulation cell is a vertex of the cell with coordinates $(0, 0, 0)$, and its replicas are defined by three indices (i_1, i_2, i_3) corresponding to a translation of the origin by the vector $i_1\vec{a}_1 + i_2\vec{a}_2 + i_3\vec{a}_3$. Then, the coordinates $\vec{r}(i')$ of the image i' of a particle $i \in \Omega$ of coordinates $\vec{r}(i)$ are given by:

$$\vec{r}(i') = \vec{r}(i) + \sum_{k=1}^{3} i_k \vec{a}_k \tag{33}$$

The particles belonging to the cell Ω, characterized by $i_1 = i_2 = i_3 = 0$, can interact with the particles of the same cell but also with image particles in the neighboring cells characterized by $i_k \in \{-1, 0, 1\}$. In D dimensions, there are $3^D - 1$ cells surrounding the simulation cell and they are involved in the search of contact partners for each particle. The distance between two particles i and $j \in \Omega$ is the shortest distance separating i from j or from one of its images j'. As the system evolves in time, a particle i may leave Ω but one of its images i' enters Ω at the same time. In order to keep all original particles in the cell Ω, the status "original" should be reserved to the particles whose centers belong to Ω. Hence, whenever a particle i leaves the simulation cell, it becomes an image of i' which then becomes original. This means that, a particle crossing a border of the simulation cell, returns to the cell by crossing another border.

The particle positions can be represented in terms of the basis vectors $\{\vec{a}_k\}$:

$$\vec{r}(i) = \sum_{k=1}^{3} s_k(i)\,\vec{a}_k = \mathbf{h}\,\vec{s}(i) \tag{34}$$

The components of $\vec{s}(i)$ define the *reduced coordinates* of particle i. For the original particles, these coordinates range from 0 to 1, corresponding thus to a point in a unitary cube. The matrix $\mathbf{h}$ transforms reduced coordinates $\vec{s}(i)$ into absolute coordinates $\vec{r}(i)$. The three columns of $\mathbf{h}$ are simply the three components of the basis vectors: $h_{kl} = (a_l)_k$.

Equation (34) shows that the position vector $\vec{r}(i)$ of a particle i can change either as a result of the variation of basis vectors $\{\vec{a}_k\}$ or due to the evolution of reduced coordinates $s_k(i)$. In the first case, the variation is homogeneous as it affects the positions of all particles in the cell whereas the second case affects only the particle i. To distinguish these two contributions, we differentiate equation (34) with respect to time:

$$\dot{\vec{r}}(i) = \dot{\mathbf{h}}\,\vec{s}(i) + \mathbf{h}\,\dot{\vec{s}}(i) \equiv \vec{u}(i) + \vec{v}(i) \tag{35}$$

The affine velocity field $\vec{u}(i) \equiv \dot{\mathbf{h}}\vec{s}(i)$ represents a homogeneous deformation of all particles. On the contrary, the velocity field $\vec{v}(i) \equiv \mathbf{h}\dot{\vec{s}}(i)$ is non-affine and describes the proper (or fluctuating) velocities of the particles with respect to a background of homogeneous deformation. Since the homogeneous deformation is carried only by the field $\vec{u}(i)$, the average value of the fluctuating part $\vec{v}(i)$ must be zero. Hence, we have

$$\langle\dot{\vec{s}}\rangle = \frac{1}{N_\mathrm{p}}\sum_{i=1}^{N_\mathrm{p}}\dot{\vec{s}}(i) = 0 \tag{36}$$

The reduced coordinates can be used to track the image particles. The relations (34) and (33) imply

$$s_k(i') = s_k(i) + i_k \tag{37}$$

Therefore, the reduced coordinates of the image particles in the neighboring cells are simply obtained by unit translations along the three space directions $k = 1, 2, 3$.

Deriving equation (37) with respect to time, we get

$$\dot{s}_k(i') = \dot{s}_k(i) \tag{38}$$

which means that the reduced velocities are periodic. As a consequence, the non-affine velocities are strictly periodic:

$$\vec{v}(i') = \mathbf{h}\dot{\vec{s}}(i') = \mathbf{h}\dot{\vec{s}}(i) = \vec{v}(i) \tag{39}$$

By definition, the affine velocities are non-periodic. Indeed, we have

$$u_k(i') = \sum_l \dot{h}_{kl}\, s_l(i') = \sum_l \dot{h}_{kl}\,(s_l(i) + i_l) = u_k(i) + \sum_l \dot{h}_{kl}\, i_l \tag{40}$$

For the calculation of relative velocities at the contact point between an original particle and an image particle, one should thus take this affine transformation of the velocities into account.

The velocity gradient tensor $\dot{\mathbf{L}}$ in the simulation cell Ω derives from the affine field $\vec{u}(i)$. By definition, we have

$$\vec{u}(i) = \dot{\mathbf{h}}\vec{s}(i) \equiv \dot{\mathbf{L}}\vec{r}(i) = \dot{\mathbf{L}}\mathbf{h}\vec{s}(i) \tag{41}$$

whence

$$\dot{\mathbf{L}} = \dot{\mathbf{h}}\,\mathbf{h}^{-1} \tag{42}$$

and the strain-rate tensor $\dot{\boldsymbol{\epsilon}}$ is the symmetric part of $\dot{\mathbf{L}}$ given by

$$\dot{\boldsymbol{\epsilon}} = \frac{1}{2}(\dot{\mathbf{L}} + \dot{\mathbf{L}}^\mathsf{T}) \tag{43}$$

where $\dot{\mathbf{L}}^\mathsf{T}$ represents the transpose of $\dot{\mathbf{L}}$.

The antisymmetric part $(\dot{\mathbf{L}} - \dot{\mathbf{L}}^\mathsf{T})/2$ corresponds to rigid rotations of the cell Ω and its replicas. However, these rotations are immaterial for a periodic system. Therefore, at least three elements (over nine) of the tensor $\dot{\mathbf{L}}$ should be fixed. For example, without loosing generality in the deformations of the simulation cell, the basis vectors $\vec{a}_1$ and $\vec{a}_2$ can be forced to remain on the plane $z = 0$ and $\vec{a}_3$ on the plane $y = 0$, so that $h_{13} = h_{23} = h_{32} = 0$. Another solution consists in canceling the antisymmetric part by imposing the velocity gradient tensor to be symmetric $\dot{\mathbf{L}} = \dot{\boldsymbol{\epsilon}}$. This implies the symmetry of the matrix $\mathbf{h}$ [47].

In addition to the particle degrees of freedom, a granular system with periodic boundary conditions has collective degrees of freedom represented by the matrix $\mathbf{h}$. We have seen that the strain-rate tensor $\dot{\boldsymbol{\epsilon}}$ (as well as the cumulative deformation tensor $\boldsymbol{\epsilon} = \int \dot{\boldsymbol{\epsilon}}\,\mathrm{d}t$) plays in practice the same role and can thus be used to represent the collective degrees of freedom. Another useful variable is the *metric tensor* $\mathbf{g}$ defined by

$$\mathbf{g} \equiv \mathbf{h}^\mathsf{T}\mathbf{h} \tag{44}$$

This tensor is symmetric and its diagonal elements describe the lengths of the three basis vectors whereas its off-diagonal elements describe the angles between those vectors [48].

The "metric" character of the tensor $\mathbf{g}$ reflects the fact that the distance $|\vec{r}(i) - \vec{r}(j)|^2$ between two particles i and j is given by

$$|\vec{r}(i) - \vec{r}(j)|^2 = \{\vec{r}(i) - \vec{r}(j)\}^\mathsf{T}\{\vec{r}(i) - \vec{r}(j)\} = \{\vec{s}(i) - \vec{s}(j)\}^\mathsf{T}\mathbf{g}\{\vec{s}(i) - \vec{s}(j)\} \tag{45}$$

Hence, the periodic system may be described by the reduced coordinates $\vec{s}(i)$ of the particles moving in a space described by the metrics $\mathbf{g}$. This is strictly equivalent to the representation of the system in terms of the absolute coordinates $\vec{r}(i)$

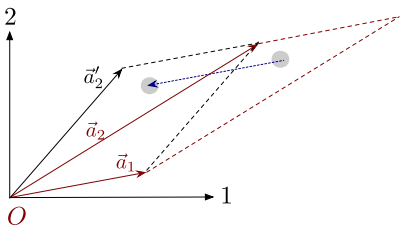

Fig. 5. Modular transformation of the cell defined by unit vectors $\{\vec{a}_1, \vec{a}_2\}$ into an equivalent cell defined by the vectors $\{\vec{a}'_1 = \vec{a}_1, \vec{a}'_2 = \vec{a}_2 - \vec{a}_1\}$.

and the matrix $\mathbf{h}$ considered as independent degrees of freedom. The evolutions of the matrix $\mathbf{h}$ and metric tensor $\mathbf{g}$ are governed by the equations of dynamics to be discussed below.

For a given configuration $\{\vec{r}(i)\}$ of the particles with their replicas, the matrix $\mathbf{h}$ can be used to obtain the reduced coordinates $\vec{s}(i) = \mathbf{h}^{-1}\vec{r}(i)$. But the definition of the simulation cell Ω, and thus that of $\mathbf{h}$, is not unique. One example is displayed in Fig. 5 where by translating a subset of particles $\in \Omega$ parallel to $-\vec{a}_1$, one obtains a new cell Ω' of the same volume as Ω and containing exactly one replica of each particle. The replicas of the new cell Ω' tesselate the space as do those of Ω. The basis vectors in this "modular" transformation change from $\{\vec{a}_1, \vec{a}_2\}$ to $\{\vec{a}_1, \vec{a}_2 - \vec{a}_1\}$.

The modular transformation, denoted by $\mathbf{T}_{\Omega'/\Omega}$, is linear:

$$\mathbf{h}' = \mathbf{T}_{\Omega'/\Omega}\mathbf{h} \tag{46}$$

The basis vectors of the matrix $\mathbf{h}$ may be modified by $\mathbf{T}$ in the course of simulation provided the velocities $\dot{\mathbf{h}}$ are transformed, too. In the example of Fig. 5, we change from the matrix $\mathbf{h} = \{\vec{a}_1, \vec{a}_2\}$ and $\dot{\mathbf{h}} = \{\dot{\vec{a}}_1, \dot{\vec{a}}_2\}$ to the matrices $\mathbf{h}' = \{\vec{a}_1, \vec{a}_2 - \vec{a}_1\}$ and $\dot{\mathbf{h}}' = \{\dot{\vec{a}}_1, \dot{\vec{a}}_2 - \dot{\vec{a}}_1\}$. These transformations should conserve the velocities $\vec{v}(i)$. Therefore the reduced coordinates and their velocities for all particles must be recalculated as $\vec{s}'(i) = \mathbf{h}'^{-1}\vec{r}'(i)$ and $\dot{\vec{s}}(i) = \mathbf{h}'^{-1}\vec{v}(i)$.

The modular transformation can be used to separate the collective dynamic variables represented by the matrix $\mathbf{h}$ from the graphical representation of the simulation cell. Indeed, $\mathbf{h}$ represents at the same time the shape of the simulation cell and collective variables of the system. But an original particle is strictly equivalent to all its images so that the calculations can be performed with the matrix $\mathbf{h}$ attributed to a cell Ω and the particles represented in another cell Ω' related to Ω by a modular transformation. For instance, let us assume that the initial cell Ω is a rectangular parallelepiped of basis vectors $\mathbf{h} = \{\vec{a}_1, \vec{a}_2, \vec{a}_3\}$. Incremental plane shearing of the system in the direction 1 transforms the cell into another parallelepiped Ω' of basis vectors $\mathbf{h}' = \{\vec{a}'_1, \vec{a}'_2\vec{a}'_3\}$ defined by $\vec{a}'_3 = \vec{a}_3$, $\vec{a}'_1 = \alpha\vec{a}_1$, $\vec{a}'_2 = \nu\vec{a}_1 + \beta\vec{a}_2$, that corresponds to the elongations α and β along the directions 1 and 2, together with shearing β along the direction 1. Obviously, the deformed cell Ω' is the modular transform of a cell Ω'' characterized by $\mathbf{h}'' = \{\vec{a}''_1, \vec{a}''_2, \vec{a}''_3\}$ with $\vec{a}''_3 = \vec{a}_3$, $\vec{a}''_1 = \alpha\vec{a}_1$, $\vec{a}'_2 = \beta\vec{a}_2$. The particles can thus be represented in the rectangular box Ω'' by applying the modular transformation $\mathbf{T}_{\Omega''/\Omega'}$. In this way, the computation is performed with $\mathbf{h}$ but the particles are represented in the rectangular cell Ω''.

These boundary conditions for shearing are known as Lee–Edwards boundary conditions [43,49,50]. As we shall see below, these limit conditions can be used alternatively with shear stress or shear strain imposed. In the same way, the cell dimensions can be fixed. In this case, considering the replicas of the simulation cell Ω'', the Lee–Edwards conditions are equivalent to rigid displacements of the neighboring cells in the direction 2 with the rates $\dot{h}_{12}h_{22}$ and $-\dot{h}_{12}h_{22}$ on the opposite sides of the central cell. This representation has the advantage of keeping the shape of the simulation cell during shear.

3.2. Dynamics

In this section, we consider the equations of motion for the particles and collective degrees of freedom by generalizing the formalism of Parrinello and Rahman to dissipative systems [44,51–53]. Let us first consider the collective degrees of freedom h_{kl} upon which depends the velocity-gradient tensor $\dot{\mathbf{L}}_{kl}$ and affine velocities $u_k(i) = \dot{h}_{kl}s_l(i)$. We assume that these variables are governed by the equations of dynamics:

$$m_h\ddot{h}_{kl} = F_{(h_{kl})} \tag{47}$$

where m_h is a "fictive mass" attached to the collective variables, and $F_{(h_{kl})}$ represents the "generalized force" associated with h_{kl}. These generalized forces are conjugate variables of h_{kl} in the sense that the rate $\dot{W}$ of the work consumed by these forces is

$$\dot{W} = \sum_{kl}\dot{h}_{kl} \cdot F_{(h_{kl})} \tag{48}$$

In order to determine $F_{(h_{kl})}$, we exploit the duality between the velocity-gradient tensor and stress tensor. Since $\dot{\mathbf{L}}$ is an Eulerian tensor, its conjugate variable is the Cauchy stress tensor $\boldsymbol{\sigma}$, which is also an Eulerian tensor. By definition, the power produced by the stresses per unit volume is the scalar product:

$$\dot{W} = V\,\dot{\mathbf{L}}\colon \boldsymbol{\sigma} \tag{49}$$

where $V = \det(\mathbf{h}) = \vec{a}_1 \cdot \vec{a}_2 \times \vec{a}_3$ is the volume of the simulation cell. Inserting the expression of $\dot{\mathbf{L}}$ given by equation (42) in (49), and given the symmetry of the stress tensor, we get

$$\dot{W} = \dot{\mathbf{h}}\colon V\mathbf{h}^{-1}\boldsymbol{\sigma} \tag{50}$$

This relation shows that $V\mathbf{h}^{-1}\boldsymbol{\sigma}$ is the conjugate variable of $\dot{\mathbf{h}}$. Hence, according to the definition (48), the generalized force is identified with

$$F_{(h_{kl})} = V(\mathbf{h}^{-1}\boldsymbol{\sigma})_{kl} \tag{51}$$

and the equation of motion of $\mathbf{h}$ becomes

$$m_h\,\ddot{\mathbf{h}} = V\mathbf{h}^{-1}\boldsymbol{\sigma} \tag{52}$$

Like the strain tensor, the stress tensor $\boldsymbol{\sigma}$ is uniform and periodic. In the same way as the matrix $\mathbf{h}$ replaces the wall degrees of freedom, the tensor $\boldsymbol{\sigma}$ plays the same role as the force on the walls. It is the sum of two terms: an external stress $\boldsymbol{\sigma}^{\mathrm{ext}}$ and an internal stress $\boldsymbol{\sigma}^{\mathrm{int}}$:

$$\boldsymbol{\sigma} = \boldsymbol{\sigma}^{\mathrm{int}} + \boldsymbol{\sigma}^{\mathrm{ext}} \tag{53}$$

With periodic boundary conditions, the internal stress $\boldsymbol{\sigma}^{\mathrm{int}}$ should be expressed from contact forces $\vec{f}$ and non-affine velocities $\vec{v}$ of the particles in the simulation cell Ω. It is given by [54–56]:

$$\boldsymbol{\sigma}^{\mathrm{int}} = n_{\mathrm{c}}\langle \boldsymbol{\ell} \otimes \mathbf{f}\rangle_{\mathrm{c}} + n_{\mathrm{p}}\langle m\boldsymbol{v} \otimes \boldsymbol{v}\rangle_{\mathrm{p}} \tag{54}$$

where n_{c} is the number density of contacts (number of contacts per unit volume), n_{p} is the number density of the particles, m is the particle mass, and $\vec{\ell}$ is the branch vector joining the centers of touching particles. The symbol $\otimes$ denotes the dyadic product. Written in terms of components, we have

$$\sigma_{kl}^{\mathrm{int}} = \frac{1}{V}\left\{\sum_{\alpha=1}^{N_{\mathrm{c}}} \ell_l(\alpha)\, f_k(\alpha) + \sum_{i=1}^{N_{\mathrm{p}}} m(i) v_k(i)\, v_l(i)\right\} \tag{55}$$

where N_{c} and N_{p} are the numbers of contacts and particles, respectively. The first average in the expression (54) runs over all contacts α inside the cell. It reflects transmission of momenta across the contact network. The second average runs over all particles i in the cell. It is simply the expression of the kinetic stress resulting from the momenta transported by the particles.

The equation of dynamics for $\mathbf{h}$ can thus be written as

$$m_h\,\ddot{\mathbf{h}} = V\mathbf{h}^{-1}(\boldsymbol{\sigma}^{\mathrm{int}} + \boldsymbol{\sigma}^{\mathrm{ext}}) \tag{56}$$

with the expression of $\boldsymbol{\sigma}^{\mathrm{int}}$ given by equation (54). Any desired mixed boundary conditions can be applied through this equation to the simulation cell. For example, for triaxial compression in the direction 3, we impose the components $\sigma_{11}^{\mathrm{ext}} = \sigma_{22}^{\mathrm{ext}}$, the velocity $\dot{h}_{33}$ and the off-diagonal terms $\dot{h}_{kl} = 0$ for $i \neq j$. According to equation (56), the resolution of the equations of dynamics yields $\sigma_{33}^{\mathrm{ext}} = -\sigma_{33}^{\mathrm{int}}$, $\sigma_{ij}^{\mathrm{ext}} = -\sigma_{ij}^{\mathrm{int}}$ for the off-diagonal terms, as well as h_{11} and h_{22} as a function of time. It is also possible to directly impose the invariants of the stress or strain tensors in all space directions by combining the equations of motion for different elements of $\mathbf{h}$ from equation (56) [40].

The Galilean invariance of a periodic system implies that the force resultants $\vec{F}(i)$ acting on the particles are strictly periodic and independent of affine velocities $\vec{u} = \dot{\mathbf{h}}\vec{s}$. For this reason, stress gradients induced by gravity or other bulk forces are incompatible with periodic conditions. The conjugate generalized velocities are thus the non-affine velocities $\vec{v}(i)$ of the particles, and the power produced by the force $\vec{F}(i)$ is given by $\dot{W}(i) = \vec{F}(i)\cdot\vec{v}(i)$. Hence, the equation of motion should involve those terms of $\ddot{\vec{r}} = \mathbf{h}\ddot{\vec{s}} + 2\dot{\mathbf{h}}\dot{\vec{s}} + \ddot{\mathbf{h}}\vec{s}$ that contribute to the variation of $\vec{v}$. These terms are $\mathbf{h}\ddot{\vec{s}}$ and $\dot{\mathbf{h}}\dot{\vec{s}} \equiv \dot{\mathbf{h}}\mathbf{h}^{-1}\vec{v} = \dot{\mathbf{L}}\vec{v}$. The only remaining term is $\ddot{\mathbf{h}}\vec{s}$ that we subtract from the acceleration $\ddot{\vec{r}}$ of the particle to get the variations of $\vec{v}$. Hence

$$\vec{F}(i) = m(i)\ddot{\vec{r}}(i) - m(i)\,\ddot{\mathbf{h}}\,\vec{s}(i) \tag{57}$$

Combining with equation (56) for $\mathbf{h}$, we get another writing of the equations of motion that does not refer to the reduced coordinates:

$$\ddot{\vec{r}}(i) = \frac{1}{m(i)}\,\vec{F}(i) + \frac{1}{m_h}\,V\,\mathbf{h}^{-1}(\boldsymbol{\sigma}^{\mathrm{int}} + \boldsymbol{\sigma}^{\mathrm{ext}})\mathbf{h}^{-1}\,\vec{r}(i) \tag{58}$$

As we shall see below, this is a convenient representation for an implicit integration scheme. It shows the coupling between the absolute degrees of freedom $\vec{r}(i)$ of the particles and the collective degrees of freedom via the second term which is proportional to the stress and depends on $\mathbf{h}$. We also note that the product $V\,(\boldsymbol{\sigma}^{\rm int}+\boldsymbol{\sigma}^{\rm ext})$ does not depend on $\mathbf{h}$.

Since the periodic deformations of the system depend only on the particle centers, the equations of dynamics for particle rotations are not affected by periodic boundary conditions. The rotations $\vec{\omega}(i)$ of the particles are thus periodic and fully disconnected from the collective degrees of freedom. They are thus governed by:

$$\vec{\tau}(i) = \boldsymbol{I}(i)\,\dot{\vec{\omega}}(i) + \vec{\omega}(i)\times\boldsymbol{I}(i)\vec{\omega}(i) \tag{59}$$

where $\vec{\tau}(i)$ is the resultant of force moments and torques acting on the particle i, and $\boldsymbol{I}$ is the moments-of-inertia matrix.

The mass m_h attributed to the collective degrees of freedom in equation (58) is an unphysical parameter. It can be compared to the wall masses when the boundary conditions are walls or clumps of particles. Since we the dynamics should represent that of a large system, the second term of the right-hand side of equation (58) should be small compared to the first term, which describes the dynamics of the particles under the action of contact forces. This means that m_h should be large with respect to $m(i)$. In particular, the relaxation time τ towards mechanical equilibrium is proportional to the square root of mass. Hence, if for the investigation of rheology we search for a well-resolved dynamics of the particles, the collective relaxation time controlled by m_h should be larger that the relaxation time of each particle controlled by its mass $m(i)$ [57,58].

4. Application to the Contact Dynamics method

The equations to be solved are those of individual particles together with those governing collective degrees of freedom. The integration scheme depends on the numerical method and its variants. For the Contact Dynamics method, it is convenient to use the writings (58) and (56) of the equations of motion. All the positions $\vec{r}$, $\vec{s}$ and $\mathbf{h}$ are treated explicitly, i.e. fixed during a time step, whereas the velocities $\dot{\vec{r}}$, $\dot{\vec{s}}$ and $\dot{\mathbf{h}}$, the contact forces $\vec{f}^{\,\alpha}$ and the un-imposed elements of the internal moment tensor $\mathbf{M}\equiv V\boldsymbol{\sigma}$ are determined through an iterative scheme. The discretized form of the equations of motion over one time step $[t, t+\delta t]$ is the following:

$$\begin{aligned}\dot{r}_k(i)[t+\delta t] &= \frac{1}{m(i)}\,\delta t\,F_k(i)[t+\delta t] + \frac{1}{m_h}\,\delta t\,P^{\rm int}_{kl}[t+\delta t]\,r_l(i)[t]\\ &\quad + B_k(i)[t]\end{aligned} \tag{60}$$

$$\dot{h}_{kl}[t+\delta t] = \frac{1}{m_h}\,\delta t\,h^{-1}_{km}[t]M^{\rm int}_{ml}[t+\delta t] + \dot{h}_{kl}[t] \tag{61}$$

$$\begin{aligned}\omega_k(i)[t+\delta t] &= \omega_k[t] + \delta t\,(I^{-1})_{kl}(i)\,\tau_l(i)[t+\delta t]\\ &\quad -(I^{-1})_{kl}(i)(\vec{\omega}(i)[t]\times\boldsymbol{I}(i)\vec{\omega}(i)[t])_l\end{aligned} \tag{62}$$

with

$$M^{\rm int}_{kl}[t+\delta t] = \sum_{\alpha=1}^{N_{\rm c}} f_k(\alpha)[t+\delta t]\ell_l(\alpha)[t] + \sum_{j=1}^{N_{\rm p}} m(j)v_k(j)[t]v_l(j)[t] \tag{63}$$

$$P^{\rm int}_{kl}[t+\delta t] = h^{-1}_{km}M^{\rm int}_{mn}[t+\delta t]h^{-1}_{nl} \tag{64}$$

$$P^{\rm ext}_{kl}[t+\delta t] = h^{-1}_{km}M^{\rm ext}_{mn}[t+\delta t]h^{-1}_{nl} \tag{65}$$

$$B_k(i)[t] = \frac{1}{m_h}\,\delta t\,P^{\rm ext}_{kl}[t]\,r_l(i)[t] + \dot{r}_k(i)[t] \tag{66}$$

where the Einstein convention for repeated symbols is assumed. Note that in this scheme the kinetic term in the expression of $\mathbf{M}^{\rm int}$ and the nonlinear term of rotations are treated explicitly.

We have seen previously that in the CD method, the equations of dynamics are condensed in the contact frames. The complementarity relations expressing Signorini's condition and Coulomb's law of friction are also written in the contact frames. With periodic boundary conditions, starting with equations (60) and (62), an iteration loop can be formed for the simultaneous determination of forces and velocities. During this iterative process, the tensor $\mathbf{M}$ is updated together with contact forces (the kinetic term kept constant during each time step).

The iterative determination of contact forces $\vec{f}^{\,\alpha}[t+\delta t]$ and internal moment tensor $M^{\rm int}_{kl}[t+\delta t]$ allows the calculation of velocities $\dot{r}_k(i)[t+\delta t]$, $\omega_k(i)[t+\delta t]$ and $\dot{h}_{kl}[t+\delta t]$ with the help of the discretized equations of motion (60), (61) and (62). The positions are updated from the velocities:

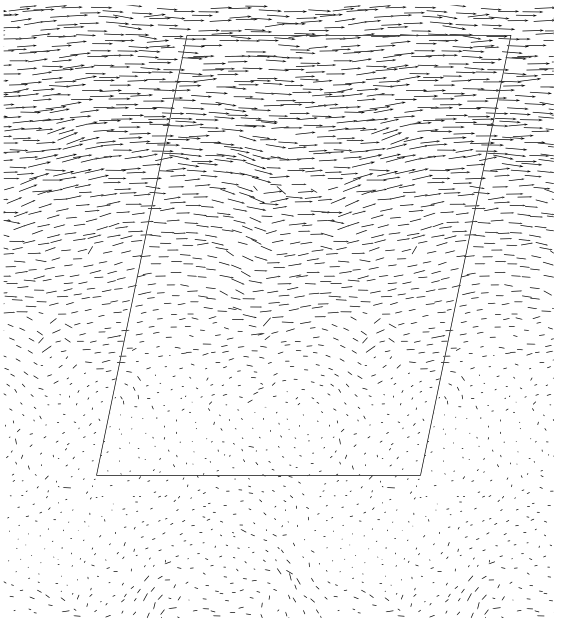

Fig. 6. A map of particle velocities in the simulation cell and neighboring cells under simple shearing with periodic boundary conditions.

$$h_{kl}[t+\delta t] = h_{kl}[t] + \delta t\, \dot{h}_{kl}[t+\delta t] \tag{67}$$

$$r_k(i)[t+\delta t] = r_k(i)[t] + \delta t\, \dot{r}_k(i)[t+\delta t] \tag{68}$$

$$\theta_k(i)[t+\delta t] = \theta_k(i)[t] + \delta t\, \omega_k(i)[t+\delta t] \tag{69}$$

For the management of periodic boundaries, we need to update the reduced positions and velocities according to the same implicit scheme:

$$\dot{s}_k(i)[t+\delta t] = (h^{-1})_{kl}[t]\,\{\dot{r}_l(i)[t+\delta t] - \dot{h}_{kl}[t+\delta t]\, s_l(i)[t]\} \tag{70}$$

$$s_k(i)[t+\delta t] = s_k(i)[t] + \delta t\, \dot{s}_k(i)[t+\delta t] \tag{71}$$

Some precautions are necessary for successful simulations with periodic boundary conditions. The round-off numerical errors in collective variables are easily amplified as they directly affect the motions of all particles. For a careful distinction between affine and non-affine velocities, it is important to satisfy the condition $\langle \dot{\vec{s}} \rangle = 0$ in spite of such round-off errors. For example, the simulation of uni-axial compaction in a given space direction under the action of an applied stress leads to an equilibrium state with $\dot{\mathbf{h}} = 0$ and $\vec{u}(i) = 0$, but a uniform displacement field $\vec{v}(i) = \mathbf{h}\dot{\vec{s}}(i) \rangle \neq 0$. In fact, it can be checked that the equation of motion is compatible with this solution, which is a consequence of Galilean invariance of the system of equations. This effect is undesirable for the analysis of the velocity field and it can be avoided by using a co-moving reference frame. In practice, it is equivalent to imposing the conditions $\langle \dot{\vec{s}} \rangle = 0$ at every time step together with the update of the particle positions and velocities.

The same issue arises with respect to the rigid rotations of the system. In fact, the stress tensor being symmetric, the antisymmetric part of the strain tensor $\dot{\mathbf{L}}$ is immaterial. Therefore, it is necessary to fix three elements of the strain tensor in 3D (one element in 2D). Another possible solution is to cancel the antisymmetric part, which leads in turn to the symmetry of the matrix $\mathbf{h}$.

5. Conclusion

The numerical simulation of granular materials with periodic boundary conditions leads to macroscopically homogeneous strains by eliminating spurious effects resulting from wall boundaries. In some cases, the rigid walls may also be replaced by membrane-like walls and other flexible elements, or by direct application of external forces and displacements on the boundary particles. The method presented in this paper is general and equivalent to the application of a homogeneous strain (affine field) and the calculation of the deviations from a homogeneous strain for the particles (non-affine field. Fig. 6 shows an example of the particle velocity field in simple shear with multi-periodic boundary conditions.

In combination with the Contact Dynamics (CD) approach, the periodic boundaries can be used to investigate the rheological behavior of granular materials composed of perfectly rigid particles interacting via frictional contacts under homogeneous conditions. We described the CD method in some detail and a general method to implement the periodic

boundary conditions. The formalism and technical details provided in this paper are essential for the CD method as, in contrast to the MD method, there is no repulsive potential acting between particles. Hence, the equations of dynamics are formulated in such as way that the affine velocities do not violate Signorini's conditions.

The periodic boundary conditions can be applied to all space directions but the same formalism may also be applied in only one direction. For example, a 2D simulation cell may be periodic in the direction x but confined by two parallel walls in the direction z. In this case, the formalism is restricted to the coordinate r_x of the particles with the corresponding matrix $\mathbf{h}$ and its reduced coordinates. One may then apply either a lateral confining stress or a lateral displacement. The case of lateral imposed displacement is trivial, involving only periodicity in position. This is a particular case of "passive" periodicity. But a general approach, as the one presented in this paper, is necessary for the application of a stress along the x direction.

Finally, it is important to remember that multi-periodic boundary conditions are fundamentally incompatible with stress gradients and shear bands as observed in real granular materials. For this reason, the periodic boundary conditions should by no means be considered as a general replacement for wall-like boundaries that occur in most practical applications. Stated differently, the multi-directional periodic boundary conditions should be used when the rheological behavior of granular materials is of interest and the mesoscopic inhomogeneities should be avoided. Such idealized conditions allow us to identify the behavior before the real boundary-value problems can be solved.

References

[1] P.A. Cundall, O.D.L. Strack, A discrete numerical model for granular assemblies, Géotechnique 29 (1) (1979) 47–65.
[2] C. Thornton, K.K. Yin, Impact of elastic spheres with and without adhesion, Powder Technol. 65 (1991) 153.
[3] H.J. Herrmann, Molecular dynamics simulations of dry granular media, in: The First Nisshin Engineering Particle Technology International Seminar: Discrete Particle Simulations in Powder Technology, Osaka, Japan, 1993, p. 8.
[4] C. Thornton, Computer simulation of impact fracture/fragmentation, in: The First Nisshin Engineering Particle Technology International Seminar: Discrete Particle Simulations in Powder Technology, Osaka, Japan, 1993, p. 17.
[5] T. Pöschel, V. Buchholtz, Molecular dynamics of arbitrarily shaped granular particles, J. Phys. I France 5 (11) (1995) 1431–1455.
[6] C. Thornton, Coefficient of restitution for collinear collisions of elastic-perfectly plastic spheres, J. Appl. Mech. 64 (1997) 383–386.
[7] S. Luding, Collisions and contacts between two particles, in: H.J. Herrmann, J.-P. Hovi, S. Luding (Eds.), Physics of Dry Granular Media, in: NATO ASI Ser., vol. E350, Kluwer Academic Publishers, Dordrecht, 1998, p. 285.
[8] H.-G. Matuttis, S. Luding, H.J. Herrmann, Discrete element methods for the simulation of dense packings and heaps made of spherical and non-spherical particles, Powder Technol. 109 (2000) 278–292.
[9] S. McNamara, H. Herrmann, Measurement of indeterminacy in packings of perfectly rigid disks, Phys. Rev. E 70 (6 Pt 1) (2004) 061303.
[10] X. Garcia, E. Medina, Acoustic response of cemented granular sedimentary rocks: molecular dynamics modeling, Phys. Rev. E, Stat. Nonlinear Soft Matter Phys. 75 (6 Pt 1) (2007) 061308.
[11] F.A. Gilabert, J.-N. Roux, A. Castellanos, Computer simulation of model cohesive powders: influence of assembling procedure and contact laws on low consolidation states, Phys. Rev. E 75 (1 Pt 1) (2007) 011303.
[12] V. Richefeu, F. Radjai, M.S.E. Youssoufi, Stress transmission in wet granular materials, Eur. Phys. J. E 21 (2007) 359–369.
[13] J.-J. Moreau, Evolution problem associated with a moving convex set in a Hilbert space, J. Differ. Equ. 26 (1977) 347–374.
[14] J.-J. Moreau, Liaisons unilatérales sans frottement et chocs inélastiques, C. R. Acad. Sci. Paris, Ser. II 296 (1983) 1473–1476.
[15] J.-J. Moreau, Bounded variation in time, in: P. Panagiotopoulos, G. Strang (Eds.), Topics in Nonsmooth Mechanics, Bikhäuser, Basel, Switzerland, 1988, pp. 1–74.
[16] J.-J. Moreau, Unilateral contact and dry friction in finite freedom dynamics, in: Nonsmooth Mechanics and Applications, in: International Centre for Mechanical Sciences, Courses and Lectures, vol. 302, Springer, Vienna, 1988, pp. 1–82.
[17] J.-J. Moreau, New computation methods in granular dynamics, in: Powders & Grains 93, A. A. Balkema, Rotterdam, The Netherlands, 1993, p. 227.
[18] J. Moreau, Some numerical methods in multibody dynamics: application to granular, Eur. J. Mech. A, Solids 13 (1994) 93–114.
[19] M. Jean, E. Pratt, A system of rigid bodies with dry friction, Int. J. Eng. Sci. (1985) 497–513.
[20] M. Jean, Unilateral contact and dry friction: time and space variables discretization, Arch. Mech. Warszawa 40 (1) (1988) 677–691.
[21] M. Jean, J.-J. Moreau, Unilaterality and dry friction in the dynamics of rigid body collections, in: Proceedings of Contact Mechanics International Symposium, Presses polytechniques et universitaires romandes, Lausanne, Switzerland, 1992, pp. 31–48.
[22] J.-J. Moreau, Numerical investigation of shear zones in granular materials, in: D.E. Wolf, P. Grassberger (Eds.), Friction, Arching, Contact Dynamics, World Scientific, Singapore, 1997, pp. 233–247.
[23] F. Radjai, M. Jean, J.-J. Moreau, S. Roux, Force distributions in dense two-dimensional granular systems, Phys. Rev. Lett. 77 (2) (1996) 274.
[24] F. Radjai, D.E. Wolf, M. Jean, J. Moreau, Bimodal character of stress transmission in granular packings, Phys. Rev. Lett. 80 (1998) 61–64.
[25] I. Bratberg, F. Radjai, A. Hansen, Dynamic rearrangements and packing regimes in randomly deposited two-dimensional granular beds, Phys. Rev. E 66 (2002) 031303.
[26] F. Radjai, S. Roux, Turbulentlike fluctuations in quasistatic flow of granular media, Phys. Rev. Lett. 89 (6) (2002) 064302.
[27] L. Staron, J.-P. Vilotte, F. Radjai, Preavalanche instabilities in a granular pile, Phys. Rev. Lett. 89 (2002) 204302.
[28] C. Nouguier-Lehon, B. Cambou, E. Vincens, Influence of particle shape and angularity on the behavior of granular materials: a numerical analysis, Int. J. Numer. Anal. Methods Geomech. 27 (2003) 1207–1226.
[29] M. Renouf, F. Dubois, P. Alart, A parallel version of the non smooth contact dynamics algorithm applied to the simulation of granular media, J. Comput. Appl. Math. 168 (1–2) (2004) 375–382.
[30] A. Taboada, K.J. Chang, F. Radjai, F. Bouchette, Rheology, force transmission, and shear instabilities in frictional granular media from biaxial numerical test using the contact dynamics method, J. Geophys. Res. 110 (2005) 1–24.
[31] G. Saussine, C. Cholet, P. Gautier, F. Dubois, C. Bohatier, J. Moreau, Modelling ballast behaviour under dynamic loading. Part 1: a 2d polygonal discrete element method approach, Comput. Methods Appl. Mech. Eng. 195 (19–22) (2006) 2841–2859.
[32] E. Azéma, F. Radjai, R. Peyroux, G. Saussine, Force transmission in a packing of pentagonal particles, Phys. Rev. E 76 (1 Pt 1) (2007) 011301.
[33] A. Ries, D.E. Wolf, T. Unger, Shear zones in granular media: three-dimensional contact dynamics simulation, Phys. Rev. E, Stat. Nonlinear Soft Matter Phys. 76 (5 Pt 1) (2007) 051301.
[34] V. Acary, M. Jean, Numerical simulation of monuments by the contact dynamics method, in: DGEMN-LNEC-JRC (Ed.), Monument-98, Workshop on Seismic Performance of Monuments, LNEC, 1998, pp. 12–14.

[35] S. Nineb, P. Alart, D. Dureisseix, Approche multi-échelle des systèmes de tenségrité, Rev. Eur. Méc. Numér. 15 (2006) 319–328.
[36] E. Radjai, R. Bideau, Stick-slip dynamics of a one-dimensional array of particles, Phys. Rev. E 52 (5) (1995) 5555–5564.
[37] F. Radjai, J. Schäfer, S. Dippel, D. Wolf, Collective friction of an array of particles: a crucial test for numerical algorithms, J. Phys. I France 7 (1997) 1053.
[38] F. Radjai, Multicontact dynamics of granular systems, Comput. Phys. Commun. 121–122 (1999) 294–298.
[39] J. Lanier, M. Jean, Experiments and numerical simulations with 2d disks assembly, Powder Technol. 109 (2000) 206–221.
[40] F. Radjai, S. Roux, Contact dynamics study of 2d granular media: critical states and relevant internal variables, in: H. Hinrichsen, D.E. Wolf (Eds.), The Physics of Granular Media, Wiley-VCH, Weinheim, Germany, 2004, pp. 165–186.
[41] S.C. McNamara, H.J. Herrmann, Quasirigidity: some uniqueness issues, Phys. Rev. E 74 (6 Pt 1) (2006) 061303.
[42] C. Thornton, L. Zhang, A DEM comparison of different shear testing devices, in: Y. Kishino (Ed.), Powders and Grains 2001, A.A. Balkema, 2001, pp. 183–190.
[43] M.P. Allen, D.J. Tildesley, Computer Simulation of Liquids, Oxford University Press, Oxford, UK, 1987.
[44] M. Parrinello, A. Rahman, Crystal structure and pair potentials: a molecular-dynamics study, Phys. Rev. Lett. 45 (1980) 1196.
[45] J. Moreau, An introduction to unilateral dynamics, in: M. Frémond, F. Maceri (Eds.), Novel Approaches in Civil Engineering, in: Lect. Notes Appl. Comput. Mech., vol. 14, Springer-Verlag, 2004, pp. 1–46.
[46] F. Radjai, V. Richefeu, Contact dynamics as a nonsmooth discrete element method, M. Mater. 41 (2009) 715–728.
[47] S. Nosé, M. Klein, Constant-temperature–constant pressure molecular-dynamics calculations for molecular solids: application to solid nitrogen at high pressure, Phys. Rev. B 33 (1986) 339–342.
[48] I. Souza, J. Martins, Metric tensor as the dynamical variable for variable-cell-shape molecular dynamics, Phys. Rev. B 55 (1997) 8733–8742.
[49] P.-E. Peyneau, J.-N. Roux, Solid-like behavior and anisotropy in rigid frictionless bead assemblies, Phys. Rev. E 78 (2008) 041307.
[50] P.-E. Peyneau, J.-N. Roux, Frictionless bead packs have macroscopic friction, but no dilatancy, Phys. Rev. E 78 (2008) 011307.
[51] M. Parrinello, A. Rahman, Polymorphic transitions in single crystals: a new molecular dynamics method, J. Appl. Phys. 52 (1981) 7182.
[52] C. Miehe, J. Dettmar, A framework for micromacro transitions in periodic particle aggregates of granular materials, Comput. Methods Appl. Mech. Eng. 193 (2004) 225–256.
[53] P. Podio-Guidugli, On (Andersen–)Parrinello–Rahman molecular dynamics, the related metadynamics, and the use of the Cauchy–Born rule, J. Elast. 100 (2010) 145–153.
[54] S.B. Savage, D.J. Jeffrey, The stress tensor in a granular flow at high shear rates, J. Fluid Mech. 110 (1981) 255.
[55] J.D. Goddard, A.K. Didwania, X. Zhuang, Computer simulations and experiment on the quasistatic mechanics and transport properties of granular materials, in: E. Guazzelli, L. Oger (Eds.), Mobile Particulate Systems, Kluwer Academic Publishers, Dordrecht, The Netherlands, 1995, p. 261.
[56] K. Bagi, Microstructural stress tensor of granular assemblies with volume forces, J. Appl. Mech. 66 (4) (1999) 934–936.
[57] I. Agnolin, J.-N. Roux, Internal states of model isotropic granular packings. I. Assembling process, geometry, and contact networks, Phys. Rev. E, Stat. Nonlinear Soft Matter Phys. 76 (6–1) (2007) 061302.
[58] I. Agnolin, J.-N. Roux, Internal states of model isotropic granular packings. II. Compression and pressure cycles, Phys. Rev. E, Stat. Nonlinear Soft Matter Phys. 76 (6–1) (2007) 061303.